




# Impact of Aging Time on the Metallurgical Properties and Hardness Characteristics of an Al-Si-Mg-Cr Hypoeutectic Alloy Intended for Automotive Applications

V.V. Ramalingam<sup>a</sup>, K.V. Shankar<sup>b, c, \*</sup> , B. Shankar<sup>b, c</sup>, R. Abhinandan<sup>b</sup>, A. Dineshkumar<sup>b</sup>, P.A. Adhithyan<sup>b</sup>, K. Velusamy<sup>b</sup>, A. Kapilan<sup>b</sup>, N. Sudheer<sup>b</sup>

<sup>a</sup> Department of Mechanical Engineering, Amrita School of Engineering, Amrita Vishwa Vidyapeetham, Coimbatore, 64112, India

<sup>b</sup> Department of Mechanical Engineering, Amrita Vishwa Vidyapeetham, Amritapuri, India

<sup>c</sup> Centre for Flexible Electronics and Advanced Materials, Amrita Vishwa Vidyapeetham, Amritapuri, India

Received 08.03.2024; accepted in revised form 28.05.2024; available online 12.06.2024

## Abstract

This research investigates the microstructural evolution and mechanical properties of LM25 (Al-Si-Mg) alloy and Cr-modified LM25-Cr (Al-Si-Mg-Cr) alloy. Microstructural analysis reveals distinctive  $\epsilon$ -Si phase morphologies, with Cr addition refining dendritic structures and reducing secondary dendrite arm spacing in the as-cast condition. Cr modification results in smaller-sized grains and a modified  $\epsilon$ -Si phase, enhancing nucleation sites and reducing  $\epsilon$ -Si size. Microhardness studies demonstrate significant increases in hardness for both alloys after solutionising and aging treatments. Cr-enriched alloy exhibits superior hardness due to solid solution strengthening, and prolonged aging further influences  $\epsilon$ -Si particle size and distribution. The concurrent rise in microhardness, attributed to refined dendritic structures and unique  $\epsilon$ -Si morphology, underscores the crucial role of Cr modification in tailoring the mechanical properties of aluminium alloys for specific applications.

**Keywords:** Al-Si-Mg, Microstructure, Hardness, Eutectic

## 1. Introduction

The LM25 aluminium alloys (Al-6.6Si-0.3Mg) possess diverse applications, particularly in the aerospace and automotive sectors. The increasing demand for specific material qualities such as tensile strength, yield strength, ductility, and tribological and corrosion behaviour underscores the significance of precise morphological control through meticulous composition

specification, metal casting methods, and subsequent T6 heat treatment processes [1]. The solidification rate is a crucial factor determining these aluminium alloys' properties, influencing the microstructure's coarseness and porosity.

Rapid solidification produces finer microstructures with improved mechanical and tribological characteristics [2-3]. As the automotive industry increasingly turns to aluminium and its alloys as a lightweight alternative to steel, there is a growing need for higher-strength modified Al alloys for safety-critical parts [4].



Hypoeutectic Al alloys (<12 wt% Si) are extensively utilized in automotive industries for constructing vital components like engine blocks and cylinder heads, commonly referred to as "piston alloys" [5-6]. Chromium is integrated into various Al-Mg-Si and Al-Mg-Zn groups to control grain structure, limit grain development, and prevent recrystallization during heat treatment or hot working. Adding chromium, not exceeding 0.35 wt% Cr, allows dispersoid precipitation during high-temperature heat treatments, enhancing corrosion and stress corrosion cracking behaviour [7-12].

Researchers have found that chromium inclusion in Al-Si-based cast alloys provides an alternative to iron and manganese for improving die-soldering resistance [13]. Studies have shown that chromium, like manganese, affects the plate-shaped  $\beta$ -Al<sub>5</sub>FeSi intermetallic in the inter-dendritic region of Al-Si-based casting alloys [14-17]. The addition of chromium forms BCC-structured Al<sub>3</sub>(Cr, Fe)<sub>4</sub>Si<sub>4</sub> in the inter-dendritic region [14]. Further investigations have revealed that adding chromium and iron to Al-Si piston alloys forms BCC structured  $\alpha$ -Al-(Cr, Fe)-Si intermetallic [15-18]. The effects of chromium and manganese on the heat-treating behaviour of Al-3Si-0.6Mg cast alloy have been explored, showing that including these elements allows dispersoids in the Al matrix, enhancing Vickers microhardness [19]. However, Cr-containing dispersoids may have minor hardness effects and are frequently incoherent with the aluminum matrix. Researchers have examined chromium concentration in AlSiMg alloys, discovering the precipitation of nanoscale Cr-bearing dispersoids and increased hardness [20-23].

Al-Si-Mg alloy castings exhibit excellent mechanical properties at room temperature, making them suitable for the transportation industry, where they often replace steel components. However, their limited wear resistance is a significant drawback. LM25 alloys, designed for specialized automotive applications, undergo alloying with various elements to enhance tribological characteristics [24-27]. Given the specific applications of Al-6.6Si-0.3Mg alloy in fabricating components for the automotive industry, such as pistons, cylinders, and cylinder heads, the current study aims to investigate the microstructural evolution and microhardness of an Al-6.6Si-0.3Mg-0.3Cr hypoeutectic alloy, focusing on the influence of aging time.

## 2. Materials and Methods

The present investigation was conducted on two alloys with composition, as shown in Table 1. The arc spectrometric analysis was employed to ascertain the chemical composition of alloys A and B. Alloy A, identified as LM25, and Alloy B, which underwent modification through the addition of chromium (0.30 wt.%), was cast by pouring molten metal at a temperature of 750°C into a metal die (Figure 1 (a)), yielding rods with dimensions of  $\phi$  32 mm in diameter and 150 mm in length, as depicted in Figure 1 (b).

Table 1.  
Chemical composition of LM 25 and Cr-modified alloy

Sample	Wt% composition								
	Al	Si	Mg	Mn	Zn	Cr	Cu	Fe	Traces
A	Bal.	6.5	0.29	0.03	0.04	Nil	0.06	0.01	0.21
B	Bal.	6.6	0.30	0.05	0.03	0.29	0.08	0.30	0.15

Subsequently, the cast rods underwent machining (Figure 1 (c)) and were subjected to a T6 heat treatment regimen. The heat treatment involved solutionizing at 538°C for 10 hours, quenching in normal water at 30°C, and aging at 175°C for varying durations of 4 hours, 8 hours, and 12 hours, with subsequent cooling in ambient air.

Specimens obtained from each condition (as-cast, solutionized, aged for 4h, aged for 8h, and aged for 12h) underwent a preparation procedure that included resin mounting and successive polishing with metallographic sheets of varying grit sizes ranging from 250 to 2000. Subsequently, the specimens were polished further using Silica OPS suspension to achieve a mirror-smooth surface. The structural characteristics were revealed through standard etching using Keller's reagent, which comprises 4% hydrofluoric acid (HF), 32% hydrochloric acid (HCl), 32% ethanol, and 32% nitric acid. Morphological imaging was performed utilizing a scanning electron microscope.

The microstructure was also captured using an optical microscope. The SDAS measurements were facilitated by image analysis software, which enabled direct length readings standardized to a microscope calibration slide. Direct SDAS measurements were taken as the length parallel to the primary arm from center to center of just two adjacent secondary arms. X-ray diffraction (XRD) analysis was conducted to elucidate the crystal structure and phases present in the specimens. Hardness assessment was carried out through Vickers microhardness testing using the Economet VH1MDX model, with a 50 g load applied for 10 seconds. Multiple measurements (10) were taken across the

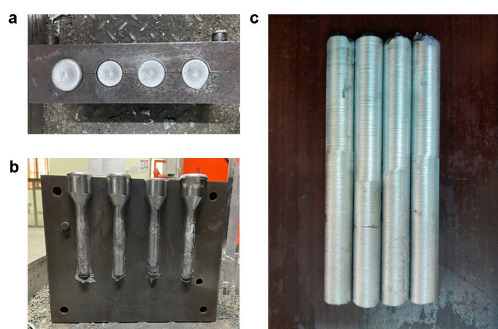


Fig. 1. Images of (a) solidification in a metal die (b) cast rods (c) machined rods

specimen surface, and the average hardness value for each specimen was calculated.

### 3. Results and discussions

#### 3.1. Morphology

Figure 2 depicts the as-cast and solutionised morphology of LM25 (Al-Si-Mg) (Figure 2a and Figure 2b), and Cr-modified LM25-Cr (Al-Si-Mg-Cr) alloy (Figure 2c and Figure 2d). The LM25 and LM25-Cr comprised the primary phase ( $\alpha$ -Al) encircled by the eutectic phase ( $\epsilon$ -Si) along the boundaries. However, a distinction was observed in the morphology and distribution of the  $\epsilon$ -Si phase. In the as-cast LM25-Cr alloy, the  $\epsilon$ -Si phase appeared to have a lamellar shape, whereas in the conventionally cast LM25 alloy, the  $\epsilon$ -Si phase had a classical form of acicular shape. Also, the distribution was homogeneous in the as-cast LM25 alloy and was along the grain boundaries in the as-cast LM25-Cr alloy.

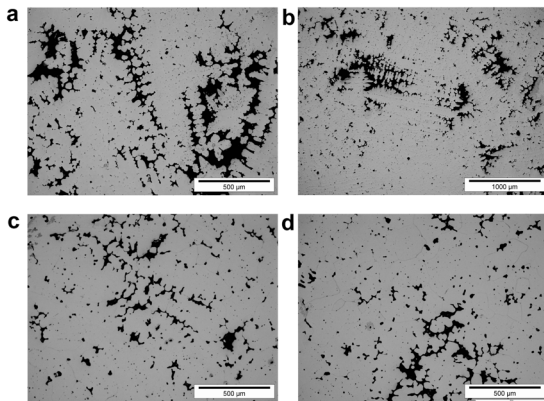


Fig. 2. Microstructure of the specimens (Optical Microscopy)

The increased shape factor observed in the LM25-Cr alloy indicates a notable enhancement in the morphology of the  $\alpha$ -Al phase. The LM25-Cr alloy exhibited a greater availability of nucleation sites, forming smaller grains than the LM25 alloy. The dendritic arm spacing (DAS) is the distance between dendritic arms that form during the solidification of a metal alloy. Adding chromium to the LM25 alloy reduced secondary dendrite arm spacing (SDAS) from 25  $\mu\text{m}$  to 14  $\mu\text{m}$  and a significant decrease in the size of the  $\epsilon$ -Si phase. Furthermore, the influence of magnesium on the growth of  $\epsilon$ -Si can be attributed to the atomic radius ratio of Mg/Si, which was approximately 1.65, a threshold considered optimal for modification.

Chromium (Cr) during solidification influenced a complex interaction of heat transfer processes occurring in both the liquid and solid phases. A significant accumulation of chromium ahead of the liquid-solid interface during solidification led to constitutional supercooling, thereby refining the dendritic structure of the alloy. The addition of chromium increased undercooling, promoting the formation of more nuclei, which

resulted in a finer structure observed in both the SDAS and the  $\epsilon$ -Si phases. In the as-cast condition, the  $\epsilon$ -Si sizes of the LM25 alloy ranged from 1-5  $\mu\text{m}$ , with an average size of 2  $\mu\text{m}$ . Upon the addition of 0.30% chromium, the  $\epsilon$ -Si size decreased to 0.1-1  $\mu\text{m}$ , with an average size of 0.5  $\mu\text{m}$ , confirming the modifying effect of chromium on the  $\epsilon$ -Si phase in the alloy.

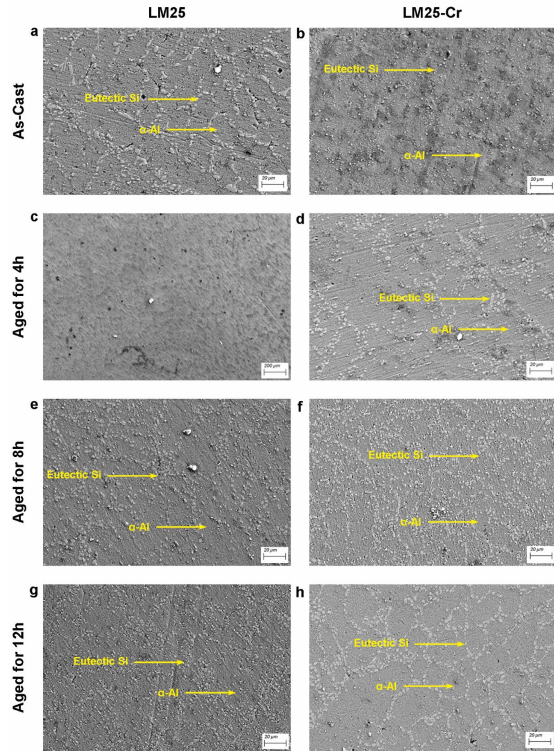


Fig. 3. Microstructure of the specimens (Scanning Electron Microscopy)

In the early stages of solution treatment heat treatment, unmodified  $\epsilon$ -Si particles experience necking and segmentation. With extended solutionizing,  $\epsilon$ -Si particles become spheroidized, resulting in a reduction in average particle size (Figure 3). The  $\epsilon$ -Si particles are already small in the as-cast state in chromium-added alloys. Consequently, the presence of twins in the silicon particles facilitates rapid branching and fragmentation during the initial phase of solution treatment, leading to accelerated spheroidization.

In the alloys enriched with 0.30% chromium, the sizes of  $\epsilon$ -Si particles exhibited a notable increase, transitioning from 0.1-1.0  $\mu\text{m}$  in the as-cast condition to 1-2  $\mu\text{m}$  after aging for 4h, with an average size of 0.5  $\mu\text{m}$ . Microstructural analyses confirmed a more spherical and diminutive  $\epsilon$ -Si shape than the LM25 alloy after 4h of aging. Following an 8h aging period, there was a further augmentation in the fraction of  $\epsilon$ -Si phases. Subsequently, the  $\epsilon$ -Si particles underwent agglomeration, increasing to 2-3  $\mu\text{m}$ , with an average size of 1.5  $\mu\text{m}$  after aging for 12h. X-ray diffraction studies confirmed that Cr did not react with Al, Mg, or Si to form intermetallic phases or compounds, as shown in Figure 4.

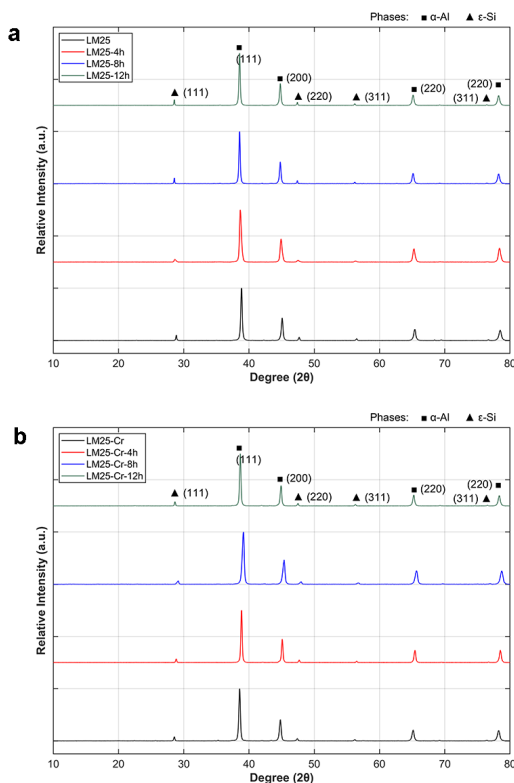


Fig. 4. Phase composition of the specimens (a) LM25 (b) LM25-Cr

### 3.2. Microhardness

Figure 5 shows the microhardness values of Al-Si-Mg and Al-Si-Mg alloy modified with Cr content. The solutionised LM25 alloy exhibited a substantial 69% increase in hardness compared to the base LM25 alloy. The increase was attributed to the dissolution of precipitates during solubilization, leading to a more homogeneous alloy and an associated enhancement in hardness.

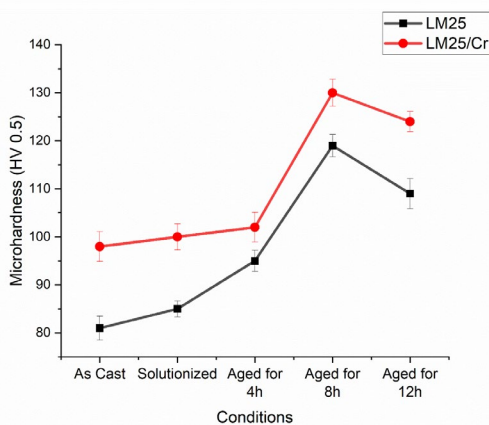


Fig. 5. Microhardness of the specimens

The impact of different aging durations was evident in the LM25-4h, LM25-8h, and LM25-12h specimens. The alloys increased hardness by 231%, 631%, and 462%, respectively, indicating that prolonged aging treatments resulted in a crest-parabolic hardening trend. The phenomenon was linked to the precipitation and growth of strengthening phases during aging, contributing to the observed hardness improvements. Incorporating Cr in the LM25 alloy resulted in a 285% increase in hardness compared to the LM25 alloy. Cr was also known for its solid solution-strengthening capabilities and played a crucial role in enhancing the overall hardness of the alloy. The subsequent solubilization treatment and further aging (LM25-Cr-4h, LM25-Cr-8h, and LM25-Cr-12h) continued to influence hardness, with notable increases of 315%, 346%, 815%, and 715%, respectively.

The alloy's arrangement and distribution of  $\alpha$ -Al and  $\epsilon$ -Si influenced its overall hardness. In the context of the LM25-Cr alloy modified with chromium, the distinctive lamellar morphology of  $\epsilon$ -Si, combined with intricately refined dendritic structures, synergistically contributed to high microhardness. The decrease in secondary dendrite arm spacing (SDAS) and the size of  $\epsilon$ -Si in LM25-Cr indicated an enhancement in the mechanical characteristics, aligning coherently with the concurrent rise in microhardness.

## 4. Conclusions

An investigation was conducted to determine the effect of ageing time on the microstructural and hardness behaviour of Al-Si-Mg and Al-Si-Mg-Cr hypoeutectic alloy and the following conclusion are presented

1. Microstructural analysis of LM25 and Cr-modified LM25-Cr alloys showed differences in  $\epsilon$ -Si phase morphology and distribution, indicating the modifying effect of chromium.
2. The addition of Cr resulted in refined dendritic structures, reduced secondary dendrite arm spacing, and smaller-sized grains, improving  $\alpha$ -Al phase morphology.
3. Heat transfer dynamics during solidification induced constitutional supercooling with Cr, further refining the dendritic structure.
4. Microhardness studies revealed substantial increases in hardness for both alloys after solutionizing and aging treatments, with Cr-enriched alloy showing enhanced hardness due to solid solution strengthening.
5. Prolonged aging affected the size and distribution of  $\epsilon$ -Si particles, emphasizing the role of alloy modification and heat treatment in tailoring mechanical properties.
6. The concurrent rise in microhardness, attributed to the synergistic contribution of refined dendritic structures and distinctive  $\epsilon$ -Si morphology, underscores the significance of chromium modification for optimizing aluminum alloy performance in specific applications.



## Conflicts of interest

The authors declare that there is no conflict of interest or competing interests for the research work.

## Funding

The authors and co-authors did not receive specific grants from any funding agency in the public, commercial, or not-for-profit sectors to carry out the research.

## References

- [1] Gustafsson, G., Thorvaldsson, T. & Dunlop, G. L. (1986). The influence of Fe and Cr on the microstructure of cast Al-Si-Mg alloys. *Metallurgical Transactions A*. 17(1), 45-52. <https://doi.org/10.1007/bf02644441>.
- [2] Liang, C., Zhao, J. F., Chang, J. & Wang, H. P. (2020). Microstructure evolution and nano-hardness modulation of rapidly solidified Ti-Al-Nb alloy. *Journal of Alloys and Compounds*. 836, 155538, 1-11. <https://doi.org/10.1016/j.jallcom.2020.155538>.
- [3] Tsepeleva, A., Novák, P., Vlášek, J. & Simoniakin, A. (2023). Use of rapid solidification in processing of aluminum alloys with reduced deep-sea nodules. *Journal of Alloys and Compounds*. 968, 171790, 1-9. <https://doi.org/10.1016/j.jallcom.2023.171790>.
- [4] Ahmad, R. (2018). The effect of chromium addition on fluidity, microstructure and mechanical properties of aluminium LM6 cast alloy. *International Journal of Material Science and Research*. 1(1), 32-35. <https://doi.org/10.18689/ijmsr-1000105>.
- [5] Zhang, G.-H., Zhang, J.-X., Li, B.-C. & Cai, W. (2011). Characterization of tensile fracture in heavily alloyed Al-Si piston alloy. *Progress in Natural Science: Materials International*. 21(5), 380-385. [https://doi.org/10.1016/s1002-0071\(12\)60073-2](https://doi.org/10.1016/s1002-0071(12)60073-2).
- [6] Barnes, S.J. & Lades, K. (2002). The evolution of aluminium based piston alloys for direct injection diesel engines. SAE Technical Paper Series.
- [7] Cole, G.S. & Sherman, A.M. (1995). Light weight materials for automotive applications. *Materials Characterization*. 35(1), 3-9. [https://doi.org/10.1016/1044-5803\(95\)00063-1](https://doi.org/10.1016/1044-5803(95)00063-1).
- [8] Strobel, K., Easton, M.A., Sweet, L., Couper, M.J., & Nie, J.-F. (2011). Relating quench sensitivity to microstructure in 6000 series aluminium alloys. *Materials Transactions*. 52(5), 914-919. <https://doi.org/10.2320/matertrans.l-mz201111>.
- [9] Yang, Y., Zhong, S.-Y., Chen, Z., Wang, M., Ma, N. & Wang, H. (2015). Effect of Cr content and heat-treatment on the high temperature strength of eutectic Al-Si alloys. *Journal of Alloys and Compounds*. 647, 63-69. <https://doi.org/10.1016/j.jallcom.2015.05.167>.
- [10] Lodgaard, L. & Ryum, N. (2000). Precipitation of dispersoids containing Mn and/or Cr in Al-Mg-Si alloys. *Materials Science & Engineering. A*. 283(1-2), 144-152. [https://doi.org/10.1016/s0921-5093\(00\)00734-6](https://doi.org/10.1016/s0921-5093(00)00734-6).
- [11] Tocci, M., Pola, A., Angella, G., Donnini, R. & Vecchia, G. M.L. (2019). Dispersion hardening of an AlSi3Mg alloy with Cr and Mn addition. *Materials Today: Proceedings*. 10, 319-326. <https://doi.org/10.1016/j.matpr.2018.10.412>.
- [12] Kim, H.Y., Han, S.W. & Lee, H.M. (2006). The influence of Mn and Cr on the tensile properties of A356-0.20Fe alloy. *Materials Letters*. 60(15), 1880-1883. <https://doi.org/10.1016/j.matlet.2005.12.042>.
- [13] Fu, Y., Wang, G.G., Hu, A., Li, Y., Thacker, K.B., Weiler, J.P. & Hu, H. (2022). Formation, characteristics and control of sludge in Al-containing magnesium alloys: An overview. *Journal of Magnesium and Alloys*. 10(3), 599-613. <https://doi.org/10.1016/j.jma.2021.11.031>.
- [14] Yamamoto, K., Takahashi, M., Kamikubo, Y., Sugiura, Y., Iwasawa, S., Nakata, T. & Kamado, S. (2020). Influence of process conditions on microstructures and mechanical properties of T5-treated 357 aluminum alloys. *Journal of Alloys and Compounds*. 834, 155133, 1-13. <https://doi.org/10.1016/j.jallcom.2020.155133>.
- [15] Callegari, B., Lima, T.N. & Coelho, R.S. (2023). The influence of alloying elements on the microstructure and properties of Al-Si-based casting alloys: A review. *Metals*, 13(7), 1174, 1-36. <https://doi.org/10.3390/met13071174>.
- [16] Silva, M.S., Barbosa, C., Acselrad, O. et al. (2004). Effect of chemical composition variation on microstructure and mechanical properties of a 6060 aluminum alloy. *Journal of Materials Engineering and Performance*. 13, 129-134. <https://doi.org/10.1361/10599490418307>.
- [17] Xiao, L., Yu, H., Qin, Y., Liu, G., Peng, Z., Tu, X., Su, H., Xiao, Y., Zhong, Q., Wang, S., Cai, Z. & Zhao, X. (2023). Microstructure and mechanical properties of cast Al-Si-Cu-Mg-Ni-Cr alloys: Effects of time and temperature on two-stage solution treatment and ageing. *Materials*. 16(7), 2675, 1-16. <https://doi.org/10.3390/ma16072675>.
- [18] Li, Y., Yang, Y., Wu, Y., Wei, Z. & Liu, X. (2011). Supportive strengthening role of Cr-rich phase on Al-Si multicomponent piston alloy at elevated temperature. *Materials Science & Engineering. A*. 528(13-14), 4427-4430. <https://doi.org/10.1016/j.msea.2011.02.047>.
- [19] Tocci, M., Donnini, R., Angella, G. & Pola, A. (2017). Effect of Cr and Mn addition and heat treatment on AlSi3Mg casting alloy. *Materials Characterization*. 123, 75-82. <https://doi.org/10.1016/j.matchar.2016.11.022>.
- [20] Engler, O. & Miller-Jupp, S. (2016). Control of second-phase particles in the Al-Mg-Mn alloy AA 5083. *Journal of Alloys and Compounds*. 689, 998-1010. <https://doi.org/10.1016/j.jallcom.2016.08.070>.
- [21] Liu, F.-Z., Qin, J., Li, Z., Yu, C.-B., Zhu, X., Nagaumi, H. & Zhang, B. (2021). Precipitation of dispersoids in Al-Mg-Si alloys with Cu addition. *Journal of Materials Research and Technology*. 14, 3134-3139. <https://doi.org/10.1016/j.jmrt.2021.08.123>.
- [22] Cui, J., Chen, J., Li, Y. & Luo, T. (2023). Enhancing the strength and toughness of A356-2.0-15Fe aluminum alloy by trace Mn and Mg Co-addition. *Metals*. 13(8), 1451, 1-12. <https://doi.org/10.3390/met13081451>.
- [23] Zhan, H. & Hu, B. (2018). Analyzing the microstructural evolution and hardening response of an Al-Si-Mg casting

- alloy with Cr addition. *Materials Characterization*. 142, 602-612. <https://doi.org/10.1016/j.matchar.2018.06.026>.
- [24] Tocci, M., Donnini, R., Angella, G. et al. (2019). Tensile Properties of a Cast Al-Si-Mg Alloy with Reduced Si Content and Cr Addition at High Temperature. *Journal of Materials Engineering and Performance*. 28, 7097-7108. <https://doi.org/10.1007/s11665-019-04438-9>.
- [25] Kumar, A., Sharma, G., Sasikumar, C., Shamim, S. & Singh, H. (2015). Effect of Cr on grain refinement and mechanical properties of Al-Si-Mg alloys. *Applied Mechanics and Materials*. 789-790, 95-99. <https://doi.org/10.4028/www.scientific.net/amm.789-790.95>.
- [26] Möller, H., Stumpf, W.E. & Pistorius, P.C. (2010). Influence of elevated Fe, Ni and Cr levels on tensile properties of SSM-HPDC Al-Si-Mg alloy F357. *Transactions of the Nonferrous Metals Society of China*. 20, 842-846. [https://doi.org/10.1016/s1003-6326\(10\)60592-4](https://doi.org/10.1016/s1003-6326(10)60592-4).
- [27] Raj, A.N. & Sellamuthu, R. (2016). Determination of hardness, mechanical and wear properties of cast Al-Mg-Si alloy with varying Ni addition. *ARPJN Journal of Engineering and Applied Science*. 11(9), 5946-5952.